THE ASTRONOMICAL JOURNAL VOLUME 104, NUMBER 5 NOVEMBER 1992

SPECTRAL-LINE BROADENING FUNCTIONS OF WUMa-TYPE BINARIES. I. AW UMa

S. M. RUCINSKI[1]

Institute for Space and Terrestrial Science and Department of Physics and Astronomy, York University, 4700 Keele Street, Toronto, Ontario M3J 1P3, Canada

Received 16 April 1992; revised 14 July 1992

ABSTRACT

We describe a method for determining the spectral-line broadening function based on simple linear mapping between sharp-line and broadline spectra that can be used when the broadening function is much narrower than the spectral window. The equations can be solved using linear least-squares techniques, with orthogonalization to remove linear dependencies resulting from the presence of featureless continuum bands in the sharp-line spectra. The broadening functions derived from high resolution, high S/N spectra of the contact binary AW UMa using our method are consistent with the contact model with the possible exception that the primary component's profiles tend to be slightly more symmetric than expected. This may indicate that the surface brightness of the inner region of the primary is lower than expected or that it has a more symmetric rotational velocity law than predicted by solid-body contact models. Fits of theoretical broadening profiles to the observed ones were used to determine the velocity scale factor, K_1+K_2, and to constrain the degree of contact of AW UMa. The primary mass is independent of the mass rato within the range $0.07<q<0.08$, but it is sensitive to the strength of the lines used to derive the radial velocity scale factor. Our best estimate of the primary mass, $\mathscr{M}_1=1.28\pm0.14\,\mathscr{M}_\odot$, suggests that AW UMa lies on the TAMS. We were unable to determine the degree of contact from our data, but we found indications that the surface of AW UMa lies close to the outer critical equipotential surface ($f\simeq0.9$).

1. INTRODUCTION

It was recognized a long time ago by Shajn & Struve (1929) that the rotational Doppler effect observed as broadening of spectral lines can be used to obtain one-dimensional maps of stars. This is the simplest of possible mapping approaches, with the spectral displacement domain being identified with the projection of the star into the velocity axis. While the idea is simple, implementations reveal a mixed degree of success. Two approaches are the most popular: the cross correlation and the Fourier-transform quotient method. In both cases broadened spectra are deconvolved using sharp-line spectra, either from slowly rotating stars or from atmosphere models. The cross-correlation method works especially well in applications which do not require the actual mapping, e.g., for precise determinations of radial velocity centroids, simultaneously for many spectral lines. As a by-product, rather crude broadening information is obtained and the method is not really a true restoration process since the resulting cross correlation contains the natural (thermal, microturbulence, etc.) broadening contributions.

The other method, the Fourier-quotient deconvolution, should be able to give the true broadening profiles as all broadening agents except the geometrical broadening are in principle removed. But this method is not as efficient as it would seem it should be because of the severe dependency on filtering in frequency space, which injects a degree of subjectivity into the whole process. Also, the restored broadening profiles sometimes contain artifacts of the process itself, such as spectral aliases and fringes which are difficult to remove. We will comment on these problems in Sec. *2.3*.

Possibly because of the difficulties of the broadening function[2] restorations, the recent interest has evolved toward techniques involving direct mapping 2D→1D using maximum entropy (for references, see, e.g., Collier Cameron & Horne 1986, Vogt *et al.* 1987, Piskunov *et al.* 1990, Maceroni *et al.* 1991, Hendry & Mochnacki 1992, Hendry *et al.* 1992). These powerful techniques base the restoration of stellar surface features on assumptions concering velocity laws (e.g., solid-body rotation) or types of spots (e.g., only dark spots), i.e., on preexisting information. In comparison, the BF restoration is conceptually much simpler and more straightforward because—in a way—the 1D mapping has already been done for us by the Doppler effect. In that respect, the broadening function has an advantage of not being able to distort information as can happen to model-dependent approaches. In fact, *it can be regarded as another way of presentation of observations*. The interpretation stage can then take place much later in the analysis process.

While identification of the velocity shift with the projected distance from the rotation axis may be legitimate in most cases, we should remember that the broadening function gives really *the intensity distribution versus radial ve-*

[1]Visiting Astronomer, Canada–France–Hawaii Telescope, operated by the National Research Council of Canada, le Centre National de la Recherche Scientifique de France, and the University of Hawaii.

[2]The term "broadening function" used throughout this paper and abbreviated BF is synonymous with the "Doppler profile" also used in the literature.

 0004-6256/92/111968-14$00.90

locity. Generally, because of the possibility of differential rotation, this does not have to be the same as the *intensity distribution versus position* on the star.

Anderson and collaborators (Anderson & Shu 1979, Anderson *et al.* 1980, Anderson *et al.* 1983) recognized that the contact binary stars of the W UMa type may be the best objects to attempt the BF restoration. The reasons are as follows: (i) the line broadening is normally very strong in these stars (of the order of ± 500 km/s) due to very short orbital periods, (ii) the surface temperature is normally almost the same over the whole contact structure, (iii) the gravity darkening is probably very small because of the subphotospheric convection. The restoration can also be used to eliminate the nonuniqueness of light-curve solutions for contact systems (Rucinski 1971). The method used by Anderson *et al.* was the Fourier-quotient deconvolution. Whereas the short study of Anderson *et al.* (1980) merely confirmed the contact model for VW Cep and rejected it for ER Vul, very interesting results were obtained by Anderson *et al.* 1983 in a thorough study of AW UMa. This system is of particular importance for an understanding of contact binaries because of its extreme mass ratio $q \simeq 0.08$. The spectral data used by Anderson *et al.* (1983) were of poor quality and it is surprising that the Fourier method worked as well as it did, but the results were significant in showing that the light distribution on AW UMa clearly deviated from the model. In particular, the primary component seemed to have a much more strongly concentrated light toward the disk center than predicted by a solid-body rotation, contact model. These important results remained unconfirmed and open to criticism (too low spectral resolution and too low S/N, spectral region with intrinsic features comparable in widths with the broadening profile, etc.). It should be noted, however, that the cross-correlation results of McLean (1981) also gave unusually narrow correlation peaks for both components of AW UMa.

Because of its extreme mass ratio, AW UMa occupies a special place among contact binaries. Yet masses of its components are poorly known because the crucial parameter, the radial velocity amplitude of the secondary component, is very difficult to measure. There are also indications that the degree of contact is unusually large for this system, possibly again because of the extreme mass ratio (Sec. 3). The present paper results from an attempt to rectify this lack of knowledge. The goal was also to confirm or disprove the Anderson *et al.* (1983) conclusions concerning the inadequacy of the contact model for AW UMa on the basis of superior, high-resolution, Reticon-coudé data from the CFH telescope. Originally, the same Fourier-quotient deconvolution technique was used but the results were not encouraging. A simple method of the BF restoration has been developed which works better in this context than the Fourier method. Section 2 describes the method and compares performance of the new method with the Fourier deconvolution. Section 3 gives results of the application of the new method to the CFHT spectra of AW UMa obtained in 1988 and 1989. Sections *3.1* and *3.2* describe the problem in general, Secs. *3.3–3.5* present the data and the derived BFs, and Secs. *3.6* and *3.7* give results obtained by applying the new BFs to improve the spectroscopic elements of AW UMa. The last, Sec. 4, gives conclusions of this work.

2. NEW METHOD OF BROADENING-FUNCTION DETERMINATION

2.1 General Description

The method presented here resulted from realization of the main deficiency of the Fourier-quotient method, when applied to the broadening-function determination. The BF is usually defined over a small range of radial velocities whereas the Fourier method provides results over the whole spectral window. The main point here is that the problem which we are dealing with is not a typical deconvolution. We are really interested in the broadening kernel, not in the deconvolved spectrum. In the language of image processing one would say that we are really interested in the PSF (point-spread function) and not in the image itself. By using the Fourier-quotient method we inefficiently extract the pertinent information because we unnecessarily determine the BF at places where we know it is equal to zero.

Thus, we would like to fulfill the following requirements.

(1) We must channel information from the whole spectral window into this section of the spectrum where the BF has some meaningful values. This can be done by setting up a system of linear equations which map the sharp-line spectra (observed for slowly rotating stars or model spectra) into the observed broadline spectra of program objects. If the spectral window is, say, 2000-pixels long and the BF is expected to be nonzero over, say, 400 pixels, the mapping has a fourfold over-determinacy $((2000-400)/400)$ which can be handled by a least-squares approach.

(2) We should realize that the sharp-line spectra with moderate numbers of lines carry little information because most of the spectrum is simply a featureless continuum of one constant value. Only real lines can be mapped into features observed in the broadened spectra. Hence, the over-determinacy is in fact much poorer than the aforementioned ratio of lengths would imply. But there is a way out of this difficulty. The least-squares process should be done in such a way as to permit orthogonalization of the data. This would ensure that only meaningful relations between sharp and broadened spectra would contribute in the mapping. Thus, sections of the continuum, which obviously produce linearly dependent basis set, would be eliminated and would not contribute to the solution. It was found that the singular value decomposition (SVD), very clearly described by Press *et al.* (1986), Sec. *2.9* solves this problem in the most elegant and simple way.

The method will be described here rather briefly. A detailed discussion of its implementation for restoration of broadening functions will appear as a separate publication in the near future.

Let's assume that we have spectra of a sharp-lined standard star, *s*, and broadened spectra of a program star, *p*,

defined at n pixels of known wavelengths. For deconvolution, the spectra must be first rebinned to radial velocity space with equal steps, ΔV. The wavelength scale corresponding to equal steps in velocity is: $\lambda_i=\lambda_0(1+\Delta V/c)^i$, $i=0,\ldots,n-1$. We used the same numbers of points in the velocity space as in the original spectra, by adjusting the size of ΔV (in km/s). Thus, we have two spectra, s_i and p_i, with the same number of elements n.

Now we should establish the convolution transformation which maps the sharp-line spectra into the broadened spectra. The aim is to determine the broadening function, b, by setting up a system of linear equations of the form: $\mathbf{S}\times\mathbf{b}=\mathbf{p}$. The vector $\mathbf{b}$ has m elements, $j=0, m-1, m<n$, and the $m\times(n-m+1)$ array $\mathbf{S}$ contains—as m columns—the appropriately shifted segments of sharp-line spectra of the same length $n-m+1$. We can place the central element of $\mathbf{b}(m_c=m/2)$ at the zero velocity by using n even and m odd. The elements of the mapping array $\mathbf{S}$ are: $S_{i,j}=s_{m+i-j-1}$, where $i=0,\ldots,n-m$ and $j=0,\ldots,m-1$. The right-hand side vector of length $n-m+1$ will have elements: p_{m_c+i}. In the array notation, the system of linear equations will be:

$$\begin{pmatrix} s_{m-1} & \cdots & s_1 & s_0 \\ s_m & \cdots & s_2 & s_1 \\ s_{m+1} & \cdots & s_3 & s_2 \\ \vdots & \vdots & \vdots & \vdots \\ s_{n-1} & \cdots & s_{n-m+1} & s_{n-m} \end{pmatrix} \begin{pmatrix} b_0 \\ b_1 \\ \vdots \\ b_{m-1} \end{pmatrix} = \begin{pmatrix} p_{m_c} \\ p_{m_c+1} \\ \vdots \\ p_{n-m_c} \end{pmatrix}. \quad (1)$$

The solution of the linear, over-determined system of equations $\mathbf{S}\times\mathbf{b}=\mathbf{p}$, for $\mathbf{b}$ requires manipulation of large arrays. Typical sizes will be of the order of $n\simeq 1000$–2000 and $m\simeq 100$–500. Thus, efficient computer methods must be used to prevent buildup of numerical errors and to ensure reasonably rapid execution. In principle, a solution can be obtained by using any least-squares approach, but we recommend that orthogonalization of the array $\mathbf{S}$ be included in the solution, perhaps as described in Sec. *2.9* of Press *et al.* (1986), using the SVD.[3] This is a very important point as an *ordinary least-squares solution will not be able to remove the linearly dependent elements of the basis set which only increase the noise but provide no useful information.*

In a very brief summary, further processing goes as follows: Both sides of Eq. (1) are multiplied by the transpose $\mathbf{S}^T$. The new $m\times m$ array $\mathbf{S}^T\mathbf{S}$ (the left-hand side of normal equations) contains information about the conditioning of our linear equation system. The SVD proceeds by splitting $\mathbf{S}^T\mathbf{S}$ into $\mathbf{U}\times\mathbf{W}\times\mathbf{V}^T$, where $\mathbf{U}$ and $\mathbf{V}^T$ are orthogonal and $\mathbf{W}$ has only diagonal elements. The solution is: $\mathbf{b}=\mathbf{V}\times[\mathrm{diag}(1/w_j)]\times(\mathbf{U}^T\times\mathbf{p})$. At this stage, removal of any linear dependences is achieved by replacement of $1/w_j$ for relatively small w_j by zero. In applying this step, we conservatively removed the diagonal elements which were smaller than 10^{-6} of the largest element. This choice is somewhat arbitrary and was dictated mostly by the level of numerical roundoff errors in single precision calculations. Our recommendation is to have the cutoff as small as tolerable to arrive at a reasonable solution but, perhaps, different cutoff levels should be tried. Since the SVD step is the most time consuming (sometimes of the order of a good fraction of an hour on Sun-4 class computers), it was found practicable to perform it with low threshold for w_j and then apply some smoothing afterwards. Indeed, in spite of the orthogonalization, the resulting vector $\mathbf{b}$ will still normally show a lot of noise and some smoothing may be necessary. However, since this step introduces some loss of information, we always keep $\mathbf{b}$ in the unsmoothed form and apply smoothing as necessary.

We should note that the process described here could easily include regularization of the solution, perhaps as described in Sec. *6.2* of Craig & Brown (1986). In case of our data, such regularization schemes did not work well, most probably because of the type of noise produced by the Reticon detectors with characteristic 4 and 8 diode patterns which remained in the data in spite of careful flat-fielding. A simple Gaussian smoothing with FWHM$\geqslant$5 pixels was found entirely satisfactory.

2.2 Example of Implementation of the Method

As an illustration, we show successive stages of analysis for one of the spectra of AW UMa obtained during the CFHT 1989 observations. These observations, as well as those obtained one year earlier, will be fully described in Sec. 3 of this paper. Here we merely show the BF solution for one spectrum, as an example that the method can work for very weak and very strongly broadened lines.

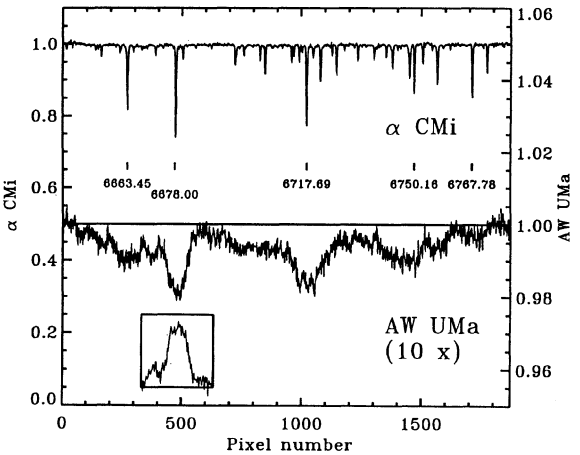

FIG. 1. Typical spectra used in the BF restoration process. The lower panel shows the spectrum of AW UMa #89-15 obtained during the 1989 CFHT run, at phase 0.792 (use the right margin scale which is expanded 10 times relative to the left-hand side scale). The upper spectrum is of Procyon, which served as a slowly rotating standard star. Both spectra have been binned to equal-velocity intervals of 3.235 km/s. The insert shows the derived BF for AW UMa at this orbital phase. The same function is shown in detail in the next Fig. 2. Here it has been plotted at arbitrary location and arbitrary vertical scale but with the correct horizontal scale, to show the relative sizes of the spectral window (1872 pixels) and of the BF (301 pixels).

[3]IDL routines were used in this study to manipulate the arrays and to perform the SVD decomposition.

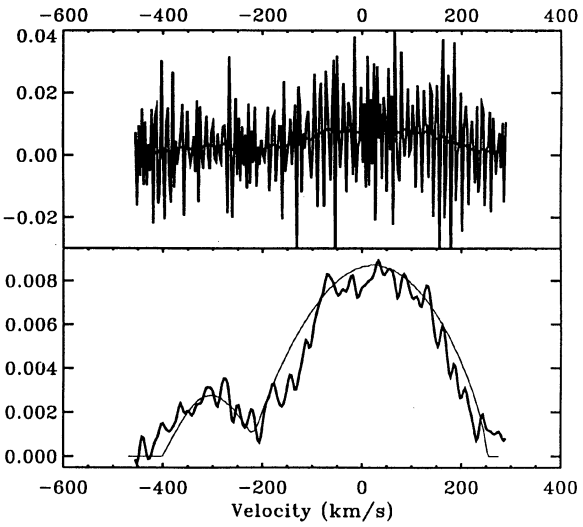

FIG. 2. Results of the SVD solution of the BF for the spectrum of AW UMa #89-15 shown in Fig. 1. The upper panel shows the raw solution which contains strong noise with the characteristic scale of 4 and 8 diodes. This noise pattern frequently remains in Reticon spectra even after careful flatfielding. Here, it became amplified in the restoration process. The "average" line running almost horizontally is the same function after smoothing with a Gaussian with FWHM=5 pixels. It is shown also in the lower panel, together with a theoretical fit for $f=0.9$ and $K_1+K_2=343$ km/s, the best fitting parameters for the 1989 data. Note that the vertical scale is in units of *intensity per resolution element* and the sum of these intensities should be close to unity (provided spectra of the program and standard stars match in equivalent line widths).

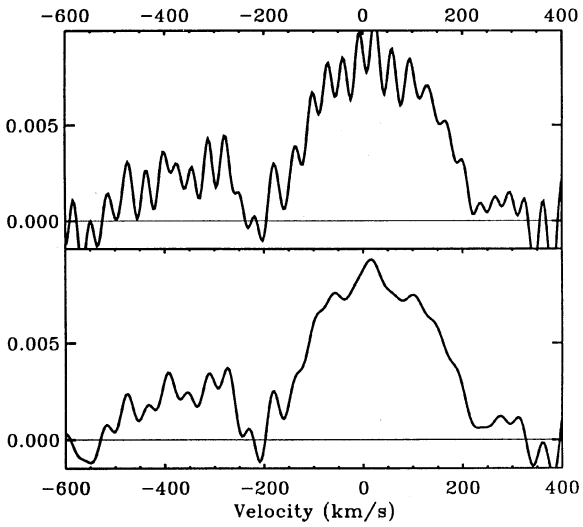

FIG. 3. Results of the Fourier-quotient deconvolution for the spectrum of AW UMa #89-15 which was shown in Fig. 1. The unfiltered result is totally dominated by noise so that only filtered results are shown. The upper panel shows results after filtering out frequencies higher than 200 cycles/window, which roughly corresponds to the resolution of the result shown in the lower panel of Fig. 2. The lower panel shows results of an even stronger filtering, down to 150 cycles/window.

Figure 1 shows the example spectrum (#89-15) of AW UMa obtained at phase 0.792 during the 1989 observing run, together with the spectrum of α CMi (Procyon) which served as a slowly rotating standard star. As we describe in Sec. 3, the spectral region selected for 1989 observations contained only weak lines. The Doppler broadening of these lines in AW UMa resulted in their very shallow depths, not exceeding 2%. Obviously, such shallow lines would be extremely difficult for any traditional spectral analysis. The spectra shown here have relatively high nominal (S/N) ratio values (per pixel), as computed from the Reticon performance data: $S/N_{AW\ UMa}\simeq 345$ (single spectrum) and $S/N_{\alpha\ CMi}\simeq 600$ (average of a few spectra).[4]

Results of the SVD least-squares solution of the broadening function are shown twice: as a small insert in Fig. 1, and in full in Fig. 2. The insert (which has been positioned in an arbitrary way close to a stronger line) illustrates the relative lengths of the full spectrum (1872 pixels) and of the restored BF (301 pixels). The interpixel spacings correspond to 3.235 km/s intervals. Figure 2 shows the solution in more detail. Its upper panel shows the solution without any smoothing. As we can see, the first impression is of very low quality result, dominated by very large noise. However, the same data, when smoothed with a Gaussian of $\sigma=3/\sqrt{2}$ pixels (corresponding to FWHM=5 pixels or 16.2 km/s) show a very reasonable result, as can be seen in the lower panel of Fig. 2.

Figure 2 shows also a theoretical fit to the observed profile which uses parameters determined for the whole set of 24 spectra of the 1989 run, as described in Sec. *3.5*. Notice, that this comparison very clearly shows the main deficiency of the method which is the need of deciding *a priori* on the length of the restored function (there is some indication of a structure for velocities beyond −400 km/s). If this function is determined over too many points, the accuracy drops; if the function is too short, some important structure at ends may be lost.

2.3 Comparison with the Fourier-Quotient Method

The Fourier-quotient technique (cf. papers by Anderson *et al.*) utilizes the well-known relationship between the integral transforms of the convolution and of the Fourier transform. The broadened profile, p, is a convolution of the sharp spectrum, s and of the broadening function, b: $p=s*b$. The Fourier transform $F\{p\}$ of the convolution is the product of the respective transforms so that b can be found, in principle, by dividing the complex transforms from: $b=F^{-1}\{F\{p\}/F\{s\}\}$.

In comparison with the method described in Sec. *2.2*, the main advantages of the Fourier method are twofold: First, the computations are faster, because of the existence of very efficient Fourier transform routines. Second, it is convenient to postpone the decision concerning the width of the restored BF for stages of the reductions as late as possible. But these advantages are offset by the well-known problems of the Fourier-quotient deconvolution. One of

[4]However, as we describe in Sec. *3.4*, every fourth pixel had to be removed due to a Reticon instrumental problem.

TABLE 1. Photometric solutions of AW UMa.

q	f	i	Solution
0.079	0.5	79.8	Mochnacki & Doughty 1972
0.0795	0.62	80.4	Lucy 1973
0.0716	0.743	79.1	Wilson & Devinney 1973
(0.0716)	0.31–0.98	(79.1)	Woodward *et al.* 1980
(0.0716)	0.44–0.87	(79.1)	Hrivnak 1982

TABLE 2. Spectroscopic solutions of AW UMa.

V_0	K_1	K_2	Author of solution
-1 ± 2	28 ± 3		Paczynski 1964
-9 ± 7	29 ± 8	423 ± 80	McLean 1981 (see text)
-0.8 ± 1.6	22.2 ± 0.9	(280 ± 30)	Rensing *et al.* 1985

those is the spatial coupling of the features, in that a single sharp peak can generate frequencies which will appear over the whole spectrum. But by far the most serious problem is amplification of the high-frequency noise in the Fourier-transform division step. Normally, this is remedied by filtering out the high frequencies. Results of such a filtering process for the same spectra as in the previous section are shown in Fig. 3. We will compare these filtered results with the SVD solution shown in Fig. 2 which involved Gaussian smoothing. Obviously, properties of a Gaussian smoothing and of a cosine smoothing (involved in removal of high frequencies) are different. Therefore, the characteristic smoothing length of FWHM=5 pixels for the Gaussian does not exactly correspond to 187 cycles per 1872 pixel spectral window. For that reason, we show results for two spectral filters, with frequencies removed above 200 cycles/window (the upper panel of Fig. 3) and above 150 cycles/window (the lower panel of Fig. 3).

As we can see by comparing Figs. 2 and 3, the new method of the BF determination described in Sec. 2 is clearly superior to the Fourier-quotient restoration. In particular, the SVD solution is free from the characteristic sinusoidal appearance of Fourier results with low-order harmonic components dominating the solution. Also, negative excursions, which frequently compensate deficiencies in restoration of positive peaks in the Fourier method, seem to be much smaller. The penalty to be paid for quality is longer computation time and the need to predetermine the size of the window for the restored function.

3. APPLICATION OF THE METHOD TO AW UMa

3.1 General Description

AW UMa (HD 99946) is a bright ($V=6.9$) contact system of spectral type F0-2 ($B-V=0.36$). It was selected as the test case for several reasons. First, it is one of the brightest W UMa type stars permitting short exposures for high resultant values of the S/N ratio. Second, it is one of the most interesting among contact binaries, having a mass ratio with the record low value of about 1:12. The secondary component is visible at all at such an extreme mass ratio only because it is a contact binary and the surface temperature is everywhere approximately the same. Third, AW UMa is one of those contact systems whose light curve can be solved very precisely because its occultation eclipse is total and of long duration. In such situations, the mass ratio (q) and inclination (i) are determined accurately without recourse to models of the surface-brightness distribution, as was demonstrated first by Mochnacki & Doughty (1972), and then confirmed by a number of subsequent geometrical elements solutions. Fourth, contrary to the excellent photometric solutions for q and i, the results on the degree of contact are discordant and the component masses are poorly known because of the difficulties with spectroscopic solutions for the secondary component. Fifth, AW UMa was already the subject of a thorough Fourier-quotient deconvolution study by Anderson *et al.* (1983) which gave quite unexpected results. The light distribution of the primary component was much more strongly concentrated than expected from the model. One could be tempted to interpret this result as lack of contact, yet the secondary component was very clearly visible, confirming beautifully the contact model. As we said before, the data used in this study were compromised by poor noise characteristics of the detector. Not only was S/N low, of the order of 10, but also the data were photographically recorded using an image tube with poor noise properties.

The main rationale of the current study was to repeat the Anderson *et al.* work using a better instrument, but otherwise keeping the remaining choices as similar as possible. This led to the 1988 CFHT observations of the same Mg I *b* triplet at 5175 Å. Problems encountered during attempts to apply the Fourier-quotient technique to these spectra were deemed to arise from large intrinsic widths and strengths of the magnesium triplet. This led to the 1989 run where a much simpler spectral region around 6700 Å was observed at the resolution two times lower. These two datasets are descibed in full below, in Secs. *3.3* and *3.4*.

3.2 Detailed Goals and Assumptions

As was mentioned above, the light curve solutions of AW UMa provide good estimates of the inclination, i, and of the mass ratio, $q=\mathcal{M}_2/\mathcal{M}_1 \leqslant 1$. The third geometrical parameter, the degree of contact (defined through distance from critical equipotentials C_1 and C_2), $f=(C_1-C)/(C_1-C_2)$, is poorly determined. We give a summary of photometric determinations in Table 1. The table does not cite the formal errors of the individual light-curve solutions which were usually unrealistically small. We can see a good external consistency of the results for q and i, whereas the determinations of f span a relatively large range between 0.3 to 1.0. The contact binaries are known to show the basically unexplained tendency for low values of f but AW UMa could be expected to have a larger value, if the proper parametrization of the degree of contact was based on the simple geometric size of the contact region, instead of that defined through equipotentials (cf. Fig. 3.1.9 in Rucinski 1985). The matter of the degree of contact has profound implications for our understanding of the physics

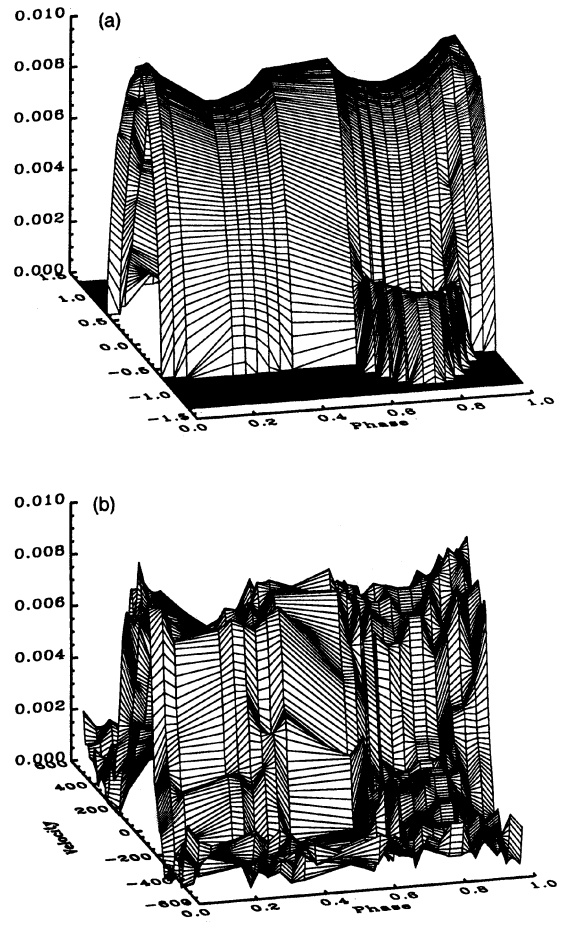

FIG. 4. The solution for AW UMa aimed at determination of parameters which are at present known with the largest uncertainty: the velocity scale for the system, K_1+K_2, and the degree of contact, f. This was done by fitting surfaces defined by theoretical BFs in the (phase, radial velocity) space to the observational results. The theoretical BFs were computed using a light curve synthesis program. In addition to K_1+K_2 and f, the systemic velocity, V_0 was determined separately from velocities of the primary component alone. Note that the fits did not involve any *vertical adjustment* of the surfaces (neither in scale or in zero point), but only selection of f and horizontal expansion/contraction of scale (with rebinning to conserve the relevant integrals). The figure shows the theoretical BFs (panel a) and the observational results (panel b) for 24 spectra obtained in 1989. The vertical scales in both cases are in the same units of *intensity per resolution element* as in Fig. 2.

TABLE 3. 1988 observations of AW UMa.

# 88–	JD (hel) 2447250+	Phase	S/N
1	0.809	0.330	137
2	0.826	0.368	133
3	0.875	0.481	107
4	0.890	0.516	114
5	0.906	0.551	114
6	0.921	0.585	128
7	0.936	0.619	138
8	0.951	0.653	154
9	0.966	0.687	142
10	0.983	0.726	152
11	0.998	0.760	146
12	1.013	0.795	134
13	1.028	0.829	117
14	1.043	0.864	125
15	1.058	0.898	92
16	1.073	0.932	78
17	2.808	0.886	102
18	2.823	0.920	129
19	2.838	0.954	118
20	2.853	0.988	119
21	2.868	0.022	126
22	2.882	0.055	120
23	2.897	0.089	134
24	2.912	0.123	129
25	2.927	0.157	136
26	2.943	0.194	140
27	2.958	0.228	125
28	2.973	0.262	115
29	2.988	0.296	112
30	3.003	0.330	109
31	3.018	0.364	94
32	3.033	0.398	86
33	3.048	0.432	88
34	3.062	0.466	76
35	3.077	0.500	52

of the contact binaries and any independent new determination of this parameter is of great value.

The spectroscopic elements of AW UMa are known rather poorly, mostly because the spectral lines of the secondary component are very difficult to measure. Thus, in the previous spectroscopic studies of Paczynski (1964) and Rensing *et al.* (1985), AW UMa was treated as a single-line binary and the radial velocity measurements were limited to the velocity amplitude of the primary, K_1. Then, through the assumed q and using $K_2=K_1/q$, the scale of the whole system, K_1+K_2, was recovered. The exception was the work of McLean (1981), who was able to measure both amplitudes, but with a very large error for K_2. The existing spectroscopic determinations are listed in Table 2. Here we do cite the rms errors because the determinations differ and are not as numerous as for the case of light-curve solutions.

We should note that the results published by Rensing *et al.* (1985) are slightly inconsistent. V_0 given in the text does not agree with that given in Table VI. After consultation with the authors, it was clarified that the table contains the correct number. Also, the result of McLean (1981) is cited with a different value than in his paper. Apparently, the published value $V_0=-17\pm7$ km/s was later modified by McLean to -9 ± 7 km/s, and this value was communicated privately to Rensing *et al.* in 1983.

The following assumptions on the parameters of AW UMa have been used throughout the present study.

(1) The inclination was fixed at $i=80°$. This parameter must be fixed as it cannot be determined by spectroscopic means.

(2) The mass ratio was fixed at $q=0.075$. The mass ratio could be considered as a free parameter. However, in this paper we actually utilize the very weak dependence of the BFs on the mass ratio within the small photometric uncertainty of less than about $\Delta q\simeq\pm0.005$ (cf. Table 1). This way, the determination of the total systemic mass

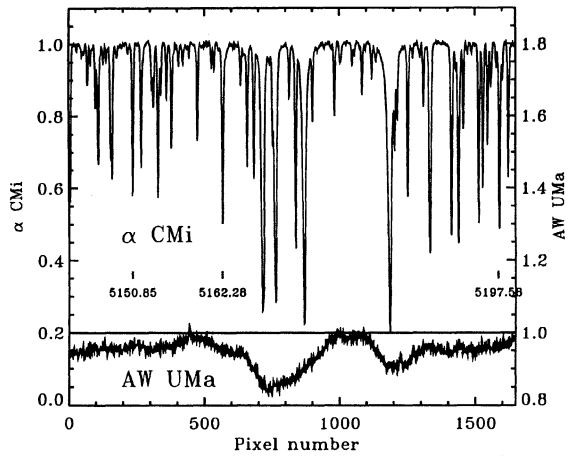

FIG. 5. A typical spectra for the 1988 CFHT run. The upper panel shows the spectrum of Procyon and the lower panel shows the spectrum of AW UMa (#88-11) at phase 0.760. This figure can be compared with Fig. 1 showing the typical spectra for the 1989 run. Note that the units of the vertical scale are the same for both panels. Notice the following features: (1) heavy blending of the lines in AW UMa, (2) considerable strengths and widths of the Mg I *b* features, (3) asymmetric positioning of the magnesium feature in the spectral window due to lack of data beyond the 1650th pixel.

(through K_1+K_2) can be decoupled from the determination of the mass ratio q.

(3) The orbital phase of the system was determined by combining the unpublished results of the recent photometric program of Derman *et al.* (1990) (the data were kindly provided by Dr. O. Demircan) with those published by Srivastava (1989) (segment $I-J$) and with one observation obtained at David Dunlap Observatory by Dr. A. Udalski (unpublished): JD (hel) = 2447549.8821. The following ephemeris was obtained: JD (hel) Pri $=2447631.0447+0.4387317\times E$.

After all computations for this paper had been concluded, the author received a manuscript by Demircan *et al.* (1992) with a discussion of the ephemeris for AW UMa. Their two new ephemerides, a linear and a quadratic one, give similar results (the linear: $2438044.8176+0.43872895\times E$, for $E>12618$). They predict moments of minima which differ from the ephemeris used here by 0.007 and 0.001 in phase for 1988 and 1989 data, respectively (our formula above giving more advanced phases). While the difference is small and even for the 1988 data amounts to about 4 min, i.e., one-fifth of a single exposure, it is nevertheless a systematic one and may affect our solution. However, it is not obvious whether the new prediction of Demircan *et al.* is the final word in this matter since it is based on data with some results somewhat arbitrarily eliminated as untrustworthy.

(4) The spectrum of α CMi (Procyon) was used as a slow rotation standard in all deconvolutions. This star has the same spectral type and color as AW UMa. This choice was tested for consistency by analyzing the total equivalent width of spectral lines in both stars (see below, Sec. *3.5* and Fig. 8). The observed equatorial velocity of α CMi, $v \sin i = 3.5 \pm 0.5$km/s(Smith 1979), is sufficiently small for the present application. The radial velocity of α CMi was assumed to be -3 km/s (the *Bright Star Catalogue*).

(5) Comparison of observations and theory was based on the standard model of contact binaries, as introduced by Lucy (1968). The synthesis program of the author (see Rucinski 1976 for references to previous papers) was used to generate the theoretical BFs by simple binning of intensities according to the projected distance from the axis of rotation. In addition to q, f, and i, the model is characterized by the gravity exponent β, as in $T_{\rm eff} \propto g^{\beta}$, and bolometric albedo, A. The "convective" values of $\beta=0.08$ and $A=0.5$ were used in most cases. The normalized BFs computed with the model were called $\mathscr{B}(y, o)$ in Anderson & Shu (1979).

At present, out of the whole set of orbital parameters of AW UMa, two parameters of AW UMa are particularly poorly known. They are: the degree of contact, f, and the velocity scale for the orbit, K_1+K_2. This study attempts to determine these parameters by searching for a least-squares minimum in the space (f, K_1+K_2) through fits of the theoretical broadening profiles to the observed ones in the 2D space (phase, radial velocity). The fits were done through least-squares searches for minimum distance between surfaces shown in Figs. 4(a) and 4(b), by adjusting the scale factor K_1+K_2 and by using the theoretical profiles for a grid of f values. The systemic velocity, V_0, was determined separately from the primary component velocities by using only the upper parts of the surfaces shown in Figs. 4 (above the 50% line for the theoretical profiles).

3.3 1988 CFHT Observations

The first series of observations of AW UMa was obtained on 1988 March 30–April 1. The coudé spectrograph and the 1872 element Reticon were used with the grating of 830 lines/mm, which gave the resolution of about 0.035 Å/diode. This corresponded to about 2 km/s at the 5175 Å Mg I "*b*" triplet. The weather was quite unstable, with clouds from time to time, so that the spectra of the same duration of 20 min had different S/N values and slightly uncertain mean times of observations. Table 3 contains the JD heliocentric time of midexposure, the phase computed from ephemeris in Sec. *3.2*, and the S/N value per diode, computed from the average strength of the signal in the spectrum. The data were subjected to the normal processing of debiasing, flatfielding, rectification, wavelength calibration, and then rebinning to the 2 km/s velocity increments. In addition to AW UMa, spectra of a few standard stars were also obtained using short exposures of a few seconds to a minute. α CMi was observed each night, to serve as the sharp-line template for the BF determinations on that night.

The data were of high quality but suffered from an instrumental problem: the shutter sometimes partly covered the diodes beyond the 1670th diode. This was an intermittent problem and the exact location of the loss of sensitivity of the detector was impossible to determine. As the result, the spectra had to be shortened to 1650 pixels. This resulted in an unfortunate loss of information and a shift of

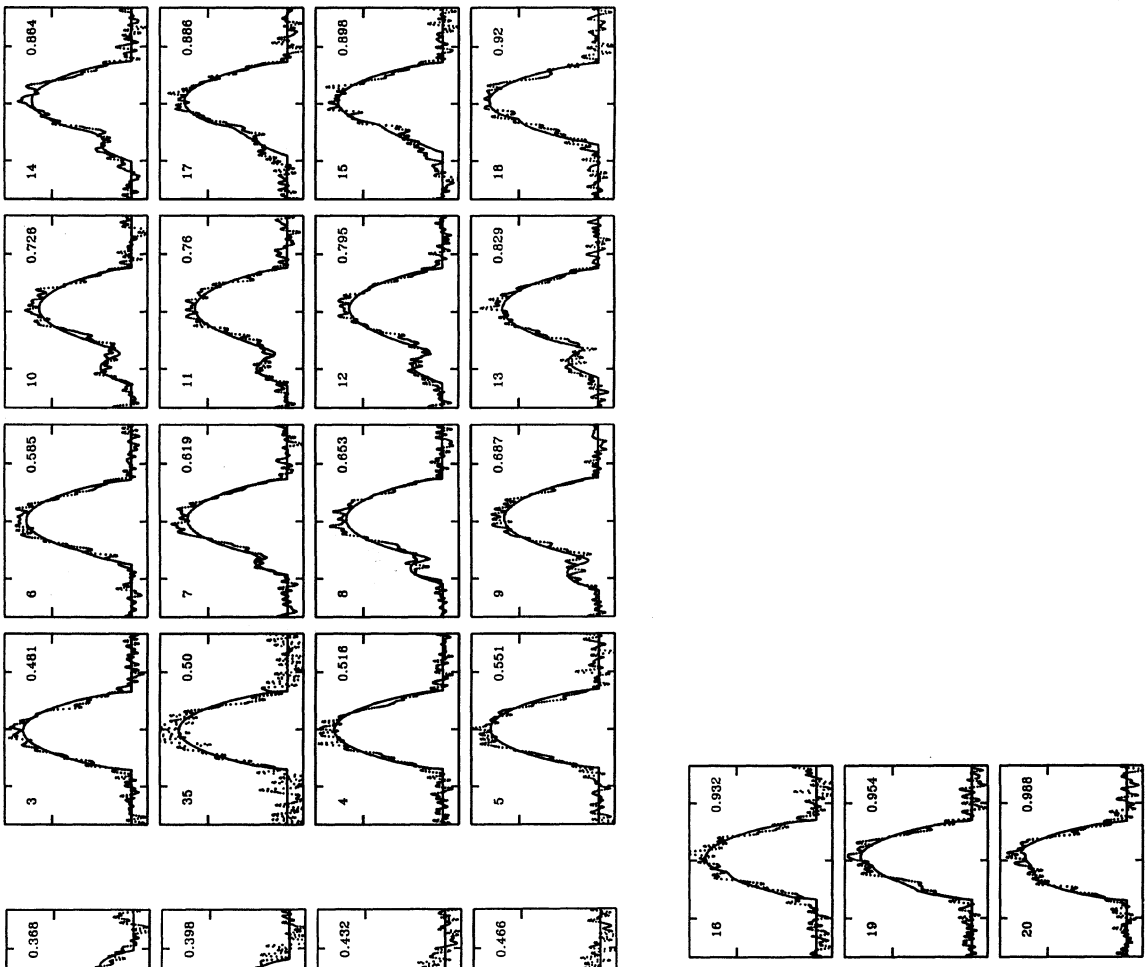

FIG. 6. Results of the BF restoration for the 1988 data. The functions are shown in panels arranged by orbital phase (numbers in the upper right corners). The consecutive numbers of spectra, as listed in Table 3, are also given (upper left corners). The continuous lines give the theoretical functions for the final set of parameters: $K_1+K_2=307$ km/s, and $f=0.9$, as discussed in Sec. *3.6*. Ticks on the horizontal scale are at -300, 0, and $+300$ km/s, and those on the vertical scale are at 0 and 0.005.

the magnesium feature from the center of the spectral window (cf. Fig. 5). Note the considerable depth of the lines and their heavy blending in the AW UMa spectra which made placement of the continuum level very difficult.

Initial attempts to use the Fourier-quotient deconvolution were not successful, mostly because the line broadening was large relative to the spectral window and because the lines were deemed too strong. Thus, the spectra were deemed useless and were put aside. Later on it became clear that the simple mapping as described in Sec. 2 worked better for the 1989 observations than the Fourier method. This led to application of the new technique to the 1988 observations which gave good results, as can be judged in Fig. 6. This figure contains a collection of all 35 BFs, arranged by phase. The BFs were obtained at 500 points, with the pixel spacing of 2 km/s. The over-determinacy $(n-m)/m$ (see Sec. 2) was only 2.3 and the results had to be smoothed. This was done by applying a Gaussian with $\sigma=3.43$ pixels, which resulted in the same resolution as the 1989 data (which were actually processed first). In velocity units the Gaussian had FWHM=16.2 km/s.

The continuous lines in each panel of Fig. 6 give model results obtained by global fitting using only three parameters: V_0, K_1+K_2, and f, with their final values, as derived in Sec. *3.6*. It should be noted that no vertical scaling was applied to the BFs and that one of the three parameters, V_0, was determined separately from velocities of the primary component alone. Thus, any freedom for adjustment really existed only in the global velocity scale factor, K_1+K_2, and in the degree of contact, f. We will return to this matter in Sec. *3.6*.

TABLE 4. 1989 observations of AW UMa.

# 89–	JD (hel) 2447630+	Phase	S/N
1	3.778	0.230	253
2	3.794	0.266	323
3	3.809	0.300	325
4	3.824	0.335	297
5	3.839	0.369	250
6	3.855	0.406	239
7	3.963	0.651	250
8	3.978	0.685	273
9	4.813	0.589	268
10	4.828	0.623	298
11	4.843	0.657	350
12	4.858	0.690	332
13	4.873	0.726	317
14	4.888	0.759	350
15	4.902	0.792	345
16	4.918	0.828	355
17	4.932	0.861	349
18	4.947	0.894	364
19	4.962	0.928	317
20	4.977	0.962	293
21	4.992	0.996	275
22	5.007	0.032	257
23	5.023	0.067	276
24	5.037	0.101	268

3.4 1989 CFHT Observations

The second series of observations was obtained on 1989 April 17, 18. The instrumental setup was the same except that this time the red channel was used, giving resolution of about 0.072 Å/diode which corresponded to about 3.235 km/s at 6700 Å. This central wavelength was selected because the spectrum is quite simple, almost empty there, and the lines are weak.

The 1989 spectra suffered from another technical problem: an extremely large, nonrepetitive, 4-diode pattern that could not be eliminated by flatfielding. This was eventually traced to the problem described by Walker *et al.* (1990). The cure was removal of one of the four Reticon channels by replacement with the averages of two neighboring pixels. This decreased the information content of the spectra by 25% and obviously still left a residual 4-diode pattern.

A typical 1989 spectrum was already shown in Fig. 1, in Sec. *2.2*. Notice the weakness of the spectral lines in the standard spectrum of Procyon and the strong broadening of lines in the spectrum of AW UMa, which is shown in Fig. 1 magnified ten times in the vertical direction relative to the scale used for α CMi.

The 1989 observations are listed in Table 4, in the same format as for the 1988 observations. All exposures for AW UMa were again 20-min long. The S/N data are per diode, estimated from the average strength of the signal. The S/N was nominally better than in 1988 because of the lower resolution, but only 75% of pixels were actually used. The weather conditions were worse than in 1988 and only 24 spectra were obtained.

The restoration process was performed in the same way as for the 1988 data. The BFs were determined over 301 points spaced by 3.235 km/s. The over-determinacy $(n-m)/m$ was 5.24. The restored functions were smoothed with a $\sigma=3/\sqrt{2}$ pixel Gaussian (FWHM=16.2 km/s). Figure 7 shows the results in the same format as in Fig. 6 and with the parameters of the theoretical fits as in Table 5.

3.5 Comparison of the 1988 and 1989 Observations

Before we discuss details of Figs. 6 and 7 which show individual BF determinations, we would like to point out that choice of α CMi as a slowly rotating standard of AW UMa was a very good one because integrals of the BFs are very close to unity. This means that the equivalent widths of lines in the spectral window were approximately the same in both stars. This is shown in Fig. 8 where some weak phase dependence is visible only in the 1988 data. Such a dependence is actually expected as the spectral type of AW UMa may change as a function of orbital phase and may be slightly later at conjunctions. It is interesting that the phase dependence is practically absent in the 1989 data and the integrals are very close to unity. We suspect, that this may be a fortuitously good result, because the 1989 data are actually more noisy. It is in fact possible that the integrated noise in 301 pixels of the BF masked the weak phase dependence and gave the almost perfect constancy of the integral.

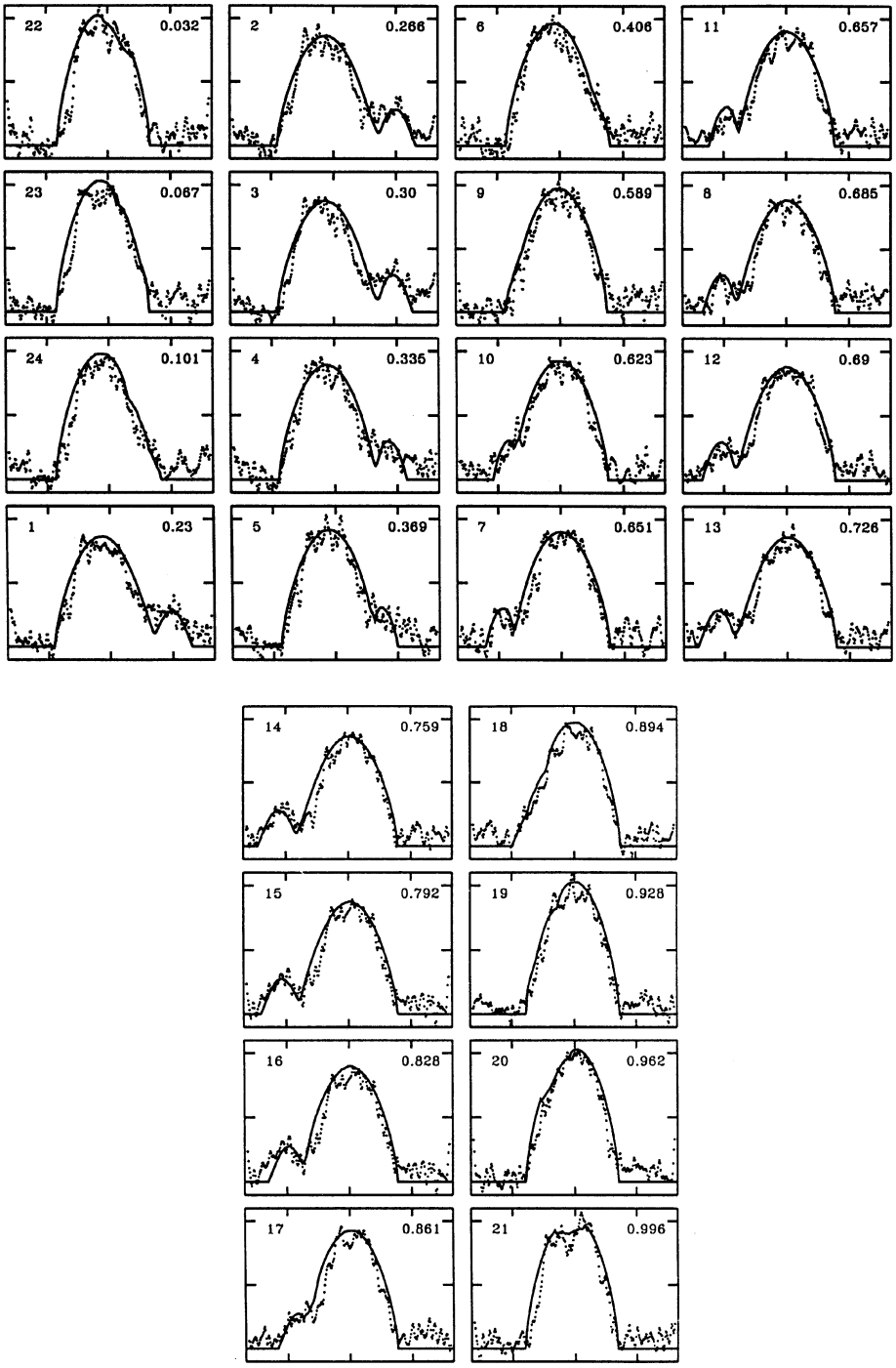

FIG. 7. Same as for Fig. 6 but for the 1989 CFHT data. The individual spectra are identified in Table 4. The continuous lines give theoretical profiles for $K_1+K_2=343$ km/s and $f=0.9$. Note the elevated base line levels of the restored BFs, especially at the right ends of the plots. Since the reason of this base line offset was unknown and its removal would be entirely arbitrary, the functions have not been corrected for it.

Comparison of the 1988 and 1989 results shows a better definition of the former, in spite of stronger intrinsic broadening of the Mg I lines and the weaker over-determinacy of the restoration process. The BFs derived from the 1988 data seem to be in good agreement with the theoretical predictions (see Fig. 6) and the only area of persistent deviations is located in the part of the primary component facing the secondary. Effectively, this corresponds to *the primary profiles being more symmetric than the contact model would predict*. This in turn may result from a number of causes; possibly, the weak gravity darkening does not apply for the primary or a dark spot is always there or, perhaps, the velocity field around the primary is symmetric relative to the rotation axis of this star. Note that the profile levels outside the main bodies are well defined and that the overall agreement in strength and shape between observations and theory for the 1988 data is amazingly good.

The 1989 results are less well defined (Fig. 7). The base line levels outside the main stellar lobes are elevated for some unknown reason and the BFs are weaker than pre-

TABLE 5. New spectroscopic parameters of AW UMa.

Value (unit)	1988	1989	Comment
V_0 (km/s) pri.	-7.1 ± 1.2	-9.5 ± 1.6*	V_0 (α CMi)=-3 km/s
f	0.9	0.9	see Fig. 10
$K_1 + K_2$ (km/s)	307 ± 11	343 ± 18	see Fig.9
$M_1 + M_2$ ($M_\odot$)	1.38 ± 0.15	1.92 ± 0.30	assumed $i = 80^0$
q	0.075	0.075	fixed, see Sec.3.2
M_1 ($M_\odot$)	1.28 ± 0.14	1.79 ± 0.28	
M_2 ($M_\odot$)	0.096 ± 0.012	0.134 ± 0.023	

*The four outlying points between phases 0.25 and 0.4 were not included. If they are included, then $V_0 = -11.6 \pm 1.7$ km/s.

dicted. The combination of these effects gives an impression that the profiles are not only weaker but also narrower than predicted by the contact model. This impression is somewhat reminiscent of the results presented by Anderson *et al.* (1983). Obviously, the disagreement between observations and prediction could be due to the genuinely weaker lines in AW UMa than in α CMi in the spectral region used in 1989. However, as we have shown above, the integrals of the BFs for 1989 data were very close to unity so that the mean equivalent widths seemed to match well. Perhaps a resolution of this inconsistency could be sought in the detrimental effects of the weakness (depth only 1%–2%) and dearth of spectral lines, and in reduced information content of spectra due to removal of 25% of pixels which could not be compensated by high S/N values.

3.6 The Parametric Fits of the Broadening Functions

Having determined the BFs at various orbital phases of AW UMa, we could attempt to improve the spectroscopic parameters for this binary system. The best-parameter searches were done only in the 2D space K_1+K_2 and f, after adjustment of the systemic velocity determined from separate (V_0, K_1) sine-curve fits to the primary component velocities. The velocities of the primary component ob-

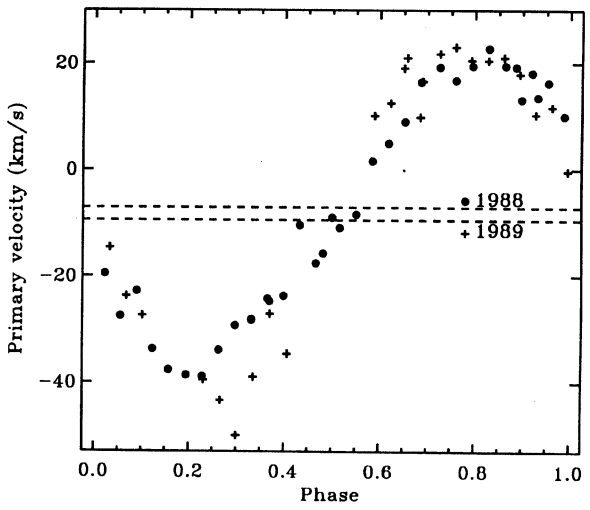

FIG. 9. Velocities of the primary component obtained by fits of the BFs truncated to the upper 50% of the profiles. The radial velocity of α CMi (-3 km/s) has been accounted for. The data obtained in 1988 (closed circles) are of better quality than in 1989 (crosses). The adopted determinations of V_0 for individual seasons are marked by broken lines. The determination for 1989 does not include the four outlying points between phases 0.25 and 0.4 (see Table 5).

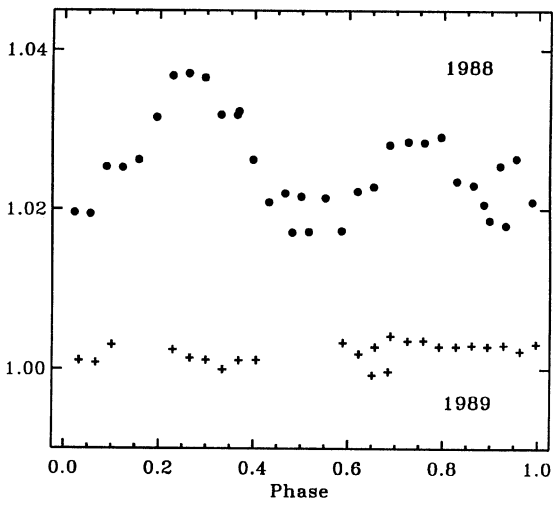

FIG. 8. Integrals of the BFs for both seasons. Closeness to unity indicates a good match of the α CMi spectrum to that of AW UMa in terms of the mean equivalent width. The phase dependence observed in 1988 (closed circles) could be either a real one, due to a spectral-type change, or could be an artifact of some hidden regularity in the continuum placement in the heavily broadened and blended spectra of AW UMa. We suspect that stability of the plot at unity for the 1989 data (crosses) is actually fortuitous (see the text).

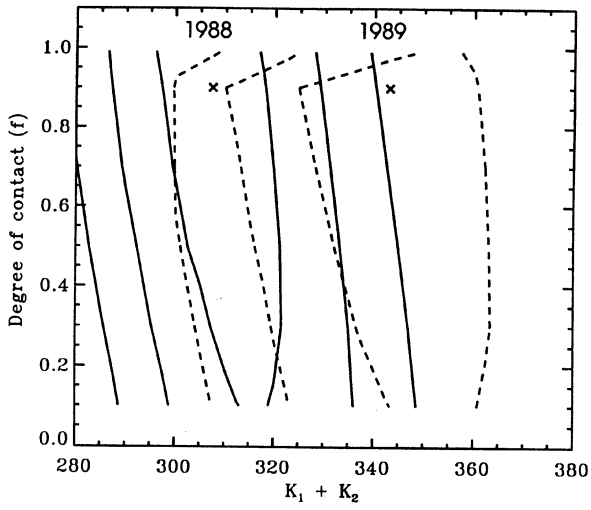

FIG. 10. Results of the K_1+K_2 and f determinations from the 1988 (continuous lines) and 1989 (broken lines) data shown as lines of equal χ^2 values (levels of 1, 2, and 3σ) in the (K_1+K_2, f) plane. The minima are marked by crosses. The shape of the 1989 minimum was asymmetric and quite shallow toward large values of K_1+K_2 so that lines for 2σ and 3σ levels are outside the figure. The χ^2 evaluation was for 2-parameter fits and included a factor of 2.3 for 1σ confidence limits (cf. the table in Sec. 14.5 in Press *et al.* 1986). The two seasonal solutions disagree at the 2–3σ level. Possibly, the disagreement reflects a deficiency in the restoration process that we are not aware of, but may also reflect a real difference in the velocity field at different atmospheric depths. However, the most likely explanation is the poorer quality of the 1989 data which manifested itself through sloping base lines of the individual BFs.

tained from profile fits to the upper 50% of the BFs are shown in Fig. 9. The by-products of the (V_0, K_1) fits, the semiamplitudes K_1 for each of the seasons, were: 28.7 ± 1.3 and 30.2 ± 1.6 km/s for 1988 and 1989, respectively. These values should not be used for determination of the component masses because they do not take into account the apparent deviations of the primary velocity from the sine curve and are inconsistent with the final determination of K_1+K_2. The values of V_0 were determined differentially relative to α CMi and then adjusted by assuming that the radial velocity of this star is -3 km/s. The determinations of V_0 for both seasons agree within their combined formal rms errors if four outlying 1989 observations are excluded (see Fig. 9). Our determinations differ from the previous determinations of Paczynski (1964) and Rensing *et al.* (1985). We have no explanation for this disagreement in V_0 but note that it has practically no influence on the final values of K_1+K_2 and hence on the determination of component masses for AW UMa.

After setting V_0 to the respective seasonal values, the BFs defined in the (phase, velocity) space were fitted by the theoretical ones through location of a minimum of $s = \Sigma w(\text{obs}-\text{theor})^2$ in the (K_1+K_2, f)-space (cf. Fig. 4). The summation is over all points of all BFs at all phases with w reflecting the adopted weighting scheme. We did not use any weights assuming that systematic errors probably dominate the random errors. For calculation of χ^2, it was assumed that the number of degrees of freedom corresponded to the number of spectra and that the fits involved two parameters. The results are shown graphically in Fig. 10 as contours of the χ^2 levels. The minima of χ^2 are located at large degrees of contact, at $f=0.9$ for both seasons, but the minima in the f coordinate are shallow and poorly defined. There is some indication that f is actually not reaching unity (i.e., outer contact) because the minimum for 1989 is asymmetric and closes up for f approaching unity. The contours in Fig. 10 give the shape of the minima at levels of 1, 2, and 3σ, where the rms error σ was calculated from $\Delta\chi^2$ confidence levels for two parameters ($\nu=2$), as described in Press *et al.* (1986, Sec. 14.5.)

It should be stressed that no additive or multiplicative corrections have been applied in the fitting process. It was felt that such corrections would bring too much arbitrariness into the process. For the same reason, the 1989 results were not corrected for elevated and slightly sloping base lines. We simply do not know what caused these offsets. Also, note that q was fixed at 0.075. Tests with theoretical profiles generated for the mass ratio of 0.07 and 0.08 indicated such a weak influence on the fits for (K_1+K_2, f), that the dependence on q could be entirely neglected at this stage.

The results of the fitting process which has lead to parameters listed in Table 5 require the following comments.

(1) Separate determinations of K_1+K_2 for each season have the 1σ halfwidths of the χ^2 minima of 11 and 18 km/s at $f=0.9$. The minimum for 1989 is shallow toward large values of K_1+K_2.

(2) There exists a disturbing difference between the 1988 and 1989 results for K_1+K_2 well beyond the 1σ levels (as estimated from the χ^2 minima). Experiments with the bootstrap-sampling solutions (multiple solutions for randomly selected observations with repetitions) gave actually smaller errors than estimates based on the shape of the χ^2 minima, which would indicate an even stronger discrepancy. In order to remain conservative, the χ^2 minimum estimates for errors of K_1+K_2 were used.

(3) The parameters K_1+K_2 and f are only weakly correlated, as can be seen in the shape of the χ^2 minima in Fig. 10.

(4) The degree of contact f is poorly determined by the data. The minima of f are located at $f=0.9$ but even 1σ uncertainty extends over the whole range of f values. There is some indication of asymmetry in the χ^2 surfaces which can be interpreted that over-contact does not actually reach the outer critical equipotential.

3.7 Spectroscopic Parameters of AW UMa

The new determinations of the total mass of AW UMa and of its components are given in Table 5. They agree very well with the result of Rensing *et al.* (1985). Our primary mass, as determined on the basis of the better 1988 data, $\mathscr{M}_1 = 1.28 \pm 0.14\ \mathscr{M}_\odot$, agrees amazingly well with the terminal age main sequence prediction of Mochnacki (1981). The 1989 data gave poorer results, with the error of $\mathscr{M}_1$ twice as big as for the 1988 observations.

The solution presented here takes full advantage of the peculiarity of AW UMa (or of any other low-q, totally eclipsing system) in that determinations of the mass ratio, q, and of the velocity scale, K_1+K_2, could be entirely decoupled. We found that choice of different q within 0.07–0.08 had no influence on our determinations K_1+K_2. At the same time, q had already been determined with high precision without any spectroscopic data. Thus, our approach was superior to that of Rensing *et al.* because their solution was in an essential way dependent on the assumption of q. They determined K_1 with high precision (22.2 ± 0.9 km/s) but then had to multiply the result by $(1+1/q)^3$ to obtain the masses.

Contrary to our initial hopes, we were not able to determine the degree-of-contact parameter f for AW UMa. We have indications that it is large but we could not determine its value. Fortunately, there seems to be very little coupling between determinations of f and K_1+K_2 (see Fig. 10) so that this uncertainty does not propagate into the mass determination.

4. CONCLUSIONS

A simple method of broadening-function determination has been presented in Sec. 2 of this paper. The method utilizes the definition of the BF as the kernel in the convolution leading from a sharp-line spectrum to the rotationally broadened spectrum. The method uses the overdetermined set of linear equations and requires handling of large arrays, so that its implementation has only recently become possible with modest computing resources. The

solution incorporates an orthogonalization step, in order to remove linear dependencies introduced by presence of the featureless continuum in the sharp-line spectrum. It was found that the SVD works particularly well for orthogonalization. The method is simple in concept and can be used for any problems requiring determination of BFs which are narrower than the used spectral window.

This paper illustrates a typical approach consisting of two steps. The first step is BF determination, in our case actually a set of determinations for various orbital phases of a binary system. This step can be considered as a simple transformation of input data, without any interpretation or implied derivations. The second step would normally involve comparison of the BFs with theory. In our case, we used theoretical predictions to improve on the spectroscopic elements of the binary system AW UMa.

The new method has been applied to two sets of the high-resolution data from CFHT (Sec. 3). Both sets were of the same contact binary, AW UMa, with the same standard star, α CMi, and both had relatively good S/N ratio. However, the data differed substantially in the choice of spectral regions and in spectral resolution (2 km/s vs 3.235 km/s, both per resolution element). The 1988 CFHT observations were of the strong, heavily blended lines and the over-determinacy of the solution (the number of usable points divided by the number of mapped points) was only 2.3. The main problem here was location of the continuum levels, which made conclusions regarding changes in the equivalent strengths of the lines uncertain (cf. Sec. *3.5* and Fig. 8). Otherwise, the results for the 1988 data are very-well defined. In contrast, the 1989 spectra covered a two-times wider region but with few, weak lines. Although the line blending was not a problem here, and the over-determinacy was higher (5.24), and there was no uncertainty with the continuum levels, the results were poorer. The BFs showed unexplained base line problem (sloping profiles), possibly related to the differences in noise characteristics between long-exposed spectra of AW UMa (20 min) and short spectra of α CMi (a few seconds).

In retrospect, one would wish to have used resolution and a spectrum region with only slightly more lines than in the 1989 data but with lines as strong as in the 1988 data.

AW UMa was selected as the first object to test the new approach because of the particularly convenient property that the BFs are practically insensitive to the mass ratio within its allowable range of $0.07 < q < 0.08$. Thus, the mass ratio and total mass determinations are basically decoupled. The former can be determined with high accuracy from photometric solutions whereas the latter requires spectroscopic data such as our BF results. Therefore, with 35 and 24 BFs at various phases for 1988 and 1989 seasons, we could attempt to solve for the velocity scale of the system, K_1+K_2, and for the degree of contact, f. These two parameters are only slightly correlated in the global solution for all phases simultaneously (cf. Fig. 10) but f could not be determined with a satisfactory accuracy. There were indications, however, that $f \simeq 0.9$, i.e., that AW UMa filled an equipotential close to the outer critical equipotential, in agreement with the previous photometric solutions. The large value of f would indicate an approximately constant geometric size of the contact region along the mass-ratio sequence (Rucinski 1985).

The main problem encountered during solutions for K_1+K_2 and f was that the determinations for 1988 and 1989 differed substantially in the velocity scale, well beyond individual formal errors. The difference may be real as the stronger lines form higher up in the atmosphere and the whole contact system may rotate differentially. However, we feel that the discrepancy may be due to the lower quality of the 1989 data. These data could have been corrected for the sloping base lines in the BFs in an *ad hoc* manner but that would introduce arbitrariness in the whole process that we wanted to avoid. In this situation, we present two independent solutions for AW UMa based on independent seasonal data (Table 5), with preference for the better defined 1988 set.

The new solution for AW UMa agrees well with that of Rensing *et al.* (1985) which, however, covered a very wide range of masses because it was very sensitive to the assumed value of the mass ratio through the factor $(1+1/q)^3$. Thus, Rensing *et al.* give the primary mass $\mathscr{M}_1 = 1.2 \pm 0.2\ \mathscr{M}_\odot$ or $\mathscr{M}_1 = 1.7 \pm 0.3\ \mathscr{M}_\odot$ assuming $q=0.07$ or $q=0.079$, respectively. Our solution for the masses does not depend on q, so we feel that our determination is intrinsically better defined. If we use only the better 1988 data and disregard the 1989 results, then $\mathscr{M}_1 = 1.28 \pm 0.14\ \mathscr{M}_\odot$. This value corresponds to the lower end of the range of masses considered for the AW UMa primary and indicates that it is an evolved object, close to the TAMS locus (Mochnacki 1981).

Finally, we would like to stress that the BFs obtained at different orbital phases of AW UMa show a very good agreement between theory and observations. Detailed comparisons of profiles, shown in Figs. 6 and 7, indicate in fact a much better agreement than in the Anderson *et al.* (1983) study. The contact model is fully confirmed and the only possible area of slight discrepancy may be the inner part of the primary profile which seems to be more symmetric than the contact model would predict. This is a very small discrepancy that we could not quantify. If it is real, it could indicate one of the following: Either the surface brightness in the inner part of the primary is lower or, the law governing surface velocities on the primary is more like that for a single, rapidly rotating star (i.e., symmetric relative to star's own axis) rather than for a solid-body rotating contact binary. We leave this point for further, more accurate and detailed studies.

The author would like to thank Tom Bolton and Andrzej Udalski for help during the CFHT observations and Stefan Mochnacki for discussion about AW UMa and other contact binaries. Thanks are also due to Nancy Evans, Janusz Kaluzny, Stefan Mochnacki and, especially, Tom Bolton who read, commented, and suggested numerous improvements to the manuscript. This work was supported by a grant from the National Sciences and Engineering Research Council of Canada.

REFERENCES

Anderson, L., Raff, M., & Shu, F. H. 1980, in Close Binary Stars: Observations and Interpretation, edited by M. J. Plavec *et al.* (Reidel, Dordrecht), p.485

Anderson, L., & Shu, F. H. 1979, ApJS, 40, 667

Anderson, L., Stanford, D., & Leininger, D. 1983, ApJ, 270, 200

Collier Cameron, A., & Horne, K. D. 1986, in Cool Stars, Stellar Systems and the Sun, edited by M. Zeilik and D. M. Gibson (Springer, Berlin), p. 205

Craig, I. J. D., & Brown, J. C. 1986, Inverse Problems in Astronomy: A Guide to Inversion Strategies for Remotely Sensed Data (Adam Hilger Ltd., Bristol and Boston)

Demircan, O., Derman, E., & Mÿesseroğlu, 1992, preprint

Derman, E., Demircan, O., & Mÿesseroğlu, 1990, Info. Bull. Var. Stars, 3540

Hendry, P. D., & Mochnacki, S. W. 1992, ApJ, 388, 603

Hendry, P. D., Mochnacki, S. W., & Collier Cameron, A. 1992, ApJ (in press)

Hrivnak, B. J. 1982, ApJ, 260, 744

Lucy, L. B. 1968, ApJ, 153, 877

Lucy, L. B. 1973, Ap&SS, 22, 381

Maceroni, C., van't Veer, F., & Vilhu, O. 1991, ESO Messenger (Dec.1991)

McLean, B. J. 1981, MNRAS, 195, 931

Mochnacki, S. W. 1981, ApJ, 245, 650

Mochnacki, S. W., & Doughty, N. A. 1972, MNRAS, 156, 51

Paczynski, B. 1964, AJ, 69, 124

Piskunov, N. E., Tuominen, I., & Vilhu, O. 1990, A&A, 230, 363

Press, W. H., Flannery, B. P., Teukolsky, S. A., & Vettering, W. T. 1986, Numerical Recipes, The Art of Scientific Computing (Cambridge University Press, Cambridge)

Rensing, M. J., Mochnacki, S. W., & Bolton, C. T. 1985, AJ, 90, 767

Rucinski, S. M. 1971, BAAS, 3, 237

Rucinski, S. M. 1976, PASP, 88, 777

Rucinski, S. M. 1985, in Interacting Binary Systems, edited by J. E. Pringle and R. A. Wade (Cambridge University Press, Cambridge), p. 85

Shajn, G., & Struve, O. 1929, MNRAS, 89, 222

Smith, M. A. 1979, PASP, 91, 737

Srivastava, R. K. 1989, Ap&SS, 154, 179

Vogt, S. S., Penrod, G. D., & Hatzes, A. P. 1987, ApJ, 321, 496

Walker, G., Johnson, R., Grieve, G., Glaspey, J., Salmon, D., Gregory, T., & Béland, S. 1990, Canada–France–Hawaii Telescope Bull. No. 22

Wilson, R. E., & Devinney, E. J. 1973, ApJ, 182, 539

Woodward, E. J., Koch, R. H., & Eisenhardt, P. R. 1980, AJ, 85, 50